Protoplasma (1996) 190: 25–38

PROTOPLASMA

Actin in living and fixed characean internodal cells: identification of a cortical array of fine actin strands and chloroplast actin rings

Geoffrey O. Wasteneys[1, 2, 3, *], David A. Collings[1], Brian E. S. Gunning[1, 2], Peter K. Hepler[3], and Diedrik Menzel[4]

[1] Plant Cell Biology Group, Research School of Biological Sciences and [2] Cooperative Research Centre for Plant Sciences, Australian National University, Canberra, ACT, [3] Biology Department, University of Massachusetts, Amherst, Massachusetts, and [4] Max Planck Institute for Cell Biology, Ladenburg

Received May 12, 1995
Accepted July 11, 1995

Summary. We report on the novel features of the actin cytoskeleton and its development in characean internodal cells. Images obtained by confocal laser scanning microscopy after microinjection of living cells with fluorescent derivatives of F-actin-specific phallotoxins, and by modified immunofluorescence methods using fixed cells, were mutually confirmatory at all stages of internodal cell growth. The microinjection method allowed capture of 3-dimensional images of high quality even though photobleaching and apparent loss of the probes through degradation and uptake into the vacuole made it difficult to record phallotoxin-labelled actin over long periods of time. When injected at appropriate concentrations, phallotoxins affected neither the rate of cytoplasmic streaming nor the long-term viability of cells. Recently formed internodal cells have relatively disorganized actin bundles that become oriented in the subcortical cytoplasm approximately parallel to the newly established long axis and traverse the cell through transvacuolar strands. In older cells with central vacuoles not traversed by cytoplasmic strands, subcortical bundles are organized in parallel groups that associate closely with stationary chloroplasts, now in files. The parallel arrangement and continuity of actin bundles is maintained where they pass round nodal regions of the cell, even in the absence of chloroplast files. This study reports on two novel structural features of the characean internodal actin cytoskeleton: a distinct array of actin strands near the plasma membrane that is oriented transversely during cell growth and rings of actin around the chloroplasts bordering the neutral line, the zone that separates opposing flows of endoplasm.

Keywords: *Chara*; F-actin; Immunofluorescence; Microtubule; *Nitella*; Phalloidin.

* Correspondence and reprints: Plant Cell Biology Group, Research School of Biological Sciences, The Australian National University, GPO Box 475, Canberra, ACT 2601, Australia.

Introduction

The conspicuous rotational streaming of giant internodal cells of characean algae (Corti 1774) is driven by acto-myosin based organelle motility (reviewed by Kamiya 1959, 1962; Kuroda 1990; Williamson 1992). Bundles of actin filaments, identified by decoration with heavy meromyosin (Palevitz et al. 1974, Williamson 1974, Kersey et al. 1976), immunofluorescence (Williamson and Toh 1979), and perfusion of fluorescently-labelled phallotoxins (Barak et al. 1980), lie in the interface between the motile endoplasm and the cortical gel and it is proposed that myosin-coated endoplasmic reticulum and other similarly coated organelles slide along these actin bundles to generate concerted movement of the endoplasmic components (Grolig et al. 1988, Kachar and Reese 1988).

Neither immunofluorescence (Williamson and Toh 1979, Wasteneys and Williamson 1991) nor electron microscopical observations (Nagai and Rebhun 1966; Pickett-Heaps 1967; Kachar and Reese 1988; McLean and Juniper 1988, 1993) has revealed the presence of actin systems other than the subcortical bundles. A small proportion of the subcortical bundles diverts through the chloroplast layer towards the cell periphery (Williamson et al. 1986) but these bundles are not analogous to the distinct cortical microtubule-associated array of fine actin filaments described

in many higher plant cells (Traas et al. 1987, McCurdy et al. 1989, Jung and Wernicke 1991). Furthermore, with the exception of actin rings associated with the nuclei of *Nitella* (but not found in *Chara corallina*; Wasteneys and Williamson 1991) there has been no conclusive evidence for the presence of actin filaments in the streaming endoplasm, despite earlier proposals that they exist and play a part in rotational streaming (Allen 1974).

In this article, we use confocal laser scanning microscopy to describe the distribution and organization of actin in the internodal cells of two characean genera. We compare the images obtained by microinjection of fluorescent phallotoxins into living cells with those obtained by indirect immunofluorescence using modified methods of fixation/permeabilization. Our study demonstrates that the distribution of actin in the cortex of internodal cells is much more extensive than previously described. Actin is found in a distinct cortical array that is oriented transversely in elongating cells, just as it is in higher plant cells. In addition, actin associates with the chloroplasts that border the neutral line, forming rings around individual chloroplasts.

Materials and methods

Plant culture

The species examined were collected in the southern tablelands of New South Wales, Australia. They included *Chara corallina* and *Nitella pseudoflabellata*. *N. pseudoflabellata* is a taxon with variable form, size and cultural requirements. We utilized a small, delicate variety with reduced furcation of the lateral whorls for microinjection experiments. Immunofluorescence work was mostly done with more robust variants. All material was cultured as frond explants in 2 or 5 l beakers containing a base substrate of 1% agar and filled with defined culture solutions. *C. corallina* and the delicate *N. pseudoflabellata* were cultured in a pH 7.0 solution consisting of (mM) NH_4Cl (0.07), $CaCl_2$ (0.5), $MgSO_4$ (0.4), Na_2CO_3 (0.2), KCl (0.4), K_2HPO_4 (0.002), Fe-EDTA (0.02), supplemented with the following micronutrients (μg/ml): $ZnCl_2$ (10), $MnCl_2$ (0.2), $CoCl_2$ (0.2), $CoCl_2 \cdot 6H_2O$ (0.2), CuCl (0.4), H_3BO_3 (40), $NaMoO_4 \cdot 2H_2O$ (10). The more robust forms of *N. pseudoflabellata* were cultured in the same solution but at half strength and supplemented with 2% (v/v) soil decoction that was prepared from a 10% (v/v) mixture of standard potting mix and tap water. Optimal growth was maintained by reculturing explants from the apices of fronds fortnightly.

Fluorescent phallotoxin preparation

Stock solutions of 6.6 μM fluorescein-phalloidin or Bodipy FL phallacidin (Molecular Probes Inc., Eugene, OR) were prepared in MeOH and kept at –80 °C until use. Prior to injection, small aliquote of this solution were desiccated and resuspended in 100 mM KCl to a working dilution of 0.66 μM followed by sonication (10 min) and centrifugation (5 min at 11,200 **g**).

Microinjection and analysis of fluorescent phallotoxin labelling by confocal laser scanning microscopy

Microinjection of internodal cells was as described (Wasteneys et al. 1993) for tubulin microinjection. Upon puncture of the cell with the micropipette, streaming normally stopped momentarily, a normal response to wounding that is attributed to induction of an action potential and subsequent rise of free calcium concentration (Williamson and Ashley 1984). Phallotoxin solution was then injected to provide a front of fluorescent material; once streaming resumed after a period of several seconds and the front was observed to disperse, the micropipette was withdrawn. By recording images of the fluorescent material before it became dispersed in the cytoplasm, it was possible to estimate the volume of phallotoxin that had been injected and compare this to cell volume. We usually found that injecting phallotoxin solutions equivalent to 1–2% of total cytoplasmic volume (6.6–13 nM) gave best results. Deliberate injection with highly concentrated phallotoxin was clearly harmful to the cell, causing rounding up and dislodgment of chloroplasts near the site of injection and, in severe cases, complete cessation of streaming. Normal concentrations, however, had no harmful effects on the cell. Streaming recovered to pre-injection rates and fluorescent levels were adequate for recording images. Labelling by the phallotoxin conjugate occurred immediately but loss of signal was rapid and unavoidable; such loss was partly caused by photobleaching during scanning and was especially apparent in the smaller cells examined. In addition, however, the probe was apparently sequestered in the vacuole and chloroplasts, the latter becoming inconveniently bright after several minutes. The use of the ion transport inhibitor probenecid (Sigma) impeded loss of fluorescent signal (see also Cole et al. 1991, Cleary et al. 1992) and brightening of chloroplasts and, at the 1 mM concentration used, streaming velocity was not affected. Recording images from living cells by confocal laser scanning was limited to low scanning intensity and averaging from a minimum of scans but it was still possible to collect serial optical sections without disrupting streaming or structural features.

Fluorescent images of phallotoxin labelling were collected with a MRC-600 (Bio-Rad Microscience Divisions) confocal laser scanning system coupled to a Zeiss Axiovert IM-10 as described (Cleary et al. 1992, Wasteneys et al. 1993). Excitation was at 488 nm with an argon laser attenuated with neutral density filters. Chloroplast autofluorescence was reduced with a 590 nm short pass filter. All images were recorded through a ×40 oil immersion Plan Neofluar objective, N.A. 1.30. Monochrome photographs were recorded from a high resolution screen with Ilford Pan-F film. Stereo-anaglyphs were photographed directly from the monitor with Fujichrome 400 ASA film. Colour prints were generated from transparencies by Cibachrome processing.

Immunofluorescence procedures

Perfusion fixation

Cells were fixed by vacuolar perfusion as described (Williamson et al. 1989) except that the following modified perfusion buffer that supported streaming reactivation was used: 40 mM HEPES (pH 7.5, Na^+), 400 mM mannitol, 70 mM KCl, 4.49 mM $MgCl_2$, 5 mM EGTA, 1.48 mM $CaCl_2$, 0.1% BSA (fatty acid-free, fraction V; Sigma) and 1% (w/v) polyvinylpyrrolidon-25000 (Sigma), 1 mg/ml ATP (Boehringer) (S. Liebe pers. comm.). Cells were placed in perfusion chambers and were examined before the nodes were cut off to check that they were actively streaming; if cells were not streaming at the time of cutting, streaming generally did not restart. Cells were

gently perfused with the streaming reactivation buffer until streaming resumed (usually < 30 s) and then perfused with 1% glutaraldehyde (from 25% stock; Sigma Grade I, stored at –20 °C) in the same buffer. Fixation was for 20 min, followed by two 10 min washes with glutaraldehyde-free buffer. Cells were then removed from perfusion wells, placed in phosphate buffered saline (PBS), and cut into short segments. The procedure for immunolabelling is described below.

Whole cell fixation

Frond tips were removed from culture and placed immediately in fixative solution of 1% glutaraldehyde in 50 mM PIPES (pH 7.2, K^+), with 2 mM EGTA, 2 mM $MgSO_4$ and 1 mM K_2HPO_4. During the 20 min fixation, larger internodes were cut into small sections with scissors, this procedure having been found to prevent plasmolysis. Material was washed twice for 10 min in glutaraldehyde-free fixation buffer, then mechanically permeabilized either by cutting the internodal cells into short segments or by freeze-shattering. To freeze-shatter, blotted tissue was placed between 2 glass slides which were held together with a clothes peg. The slides were plunged into liquid nitrogen approx. 10 s, removed to a pre-chilled (–80 °C) block of aluminium and pressure applied with a gloved thumb to fracture the now glass-hard tissue. A similar method has been described for permeabilizing cell walls of *Chara* rhizoids for immunofluorescence microscopy (Braun and Sievers 1994). After shattering, the tissue was thawed in permeabilization buffer (1% Triton X-100 in PBS, pH 7.4).

Immunolabelling

Fixed and permeabilized material was incubated in PBS with 1% Triton X-100 and agitated gently on a rotory shaker for 3 h. Before immunolabelling, tissue was washed twice in PBS to remove detergent, treated with 1 mg/ml $NaBH_4$ for 15 min, then incubated in antibody incubation buffer (50 mM glycine in PBS, pH 7.4) for 30 min. Primary and secondary labelling was for 1 h each with three 10 min washes with the same buffer between incubations. After secondary antibody labelling, material was washed (three times for 10 min) in PBS and mounted in 0.1% *para*-phenylene diamine and 50% glycerol in PBS, pH 9.

Antibodies

For actin labelling, clone N350 (Amersham) a mouse IgM raised against chicken gizzard actin and recognizing all non-muscle actins was used at 1 : 100. The same labelling patterns were obtained with C4 (ICN), which is also raised against chicken gizzard actin (Lessard 1988). Microtubules were labelled with clone TUB-1A2 (Sigma), at 1 : 800. Secondary antibodies included FITC conjugates from Sigma specific to mouse IgG (F-0257, used 1 : 75) and mouse IgM (F-9259, used 1 : 40).

Microscopy

Images of immunofluorescently labelled material were recorded with a prototype confocal laser scanning microscope (Leica Laser Technik, Heidelberg, Federal Republic of Germany) coupled to a standard inverted microscope (IM 35; Zeiss, Oberkochen, Federal Republic of Germany). Excitation light of 488 and 514 nm was generated by an Omnichrome argon ion laser connected to the optical path of the scanning unit via glass fibre cable. Monochrome photographs were recorded on Ilford Pan-F film using a Leica 35 mm camera mounted on a high resolution screen. Colour prints of anaglyphs were generated on a Mitsubishi CP100E colour video copy processor.

Results

Internodal cells of the whorls or branchlets that emerge at the nodal regions show similar developmental patterns to the internodal cells of the frond's central axis. In many cases, working with the smaller whorl internodal cells was more convenient. The images shown in this article document examples of both types of internode. We have also included representative examples from two characean genera, *Chara* and *Nitella*.

Subcortical actin bundles become increasingly well ordered as internodal cell elongation proceeds

The early development of internodal cells involves elongation of subapical, uni-nucleate cells into multinucleate, highly vacuolated cylinders. Streaming can be detected as soon as elongation is evident and is organized into two opposing streams of apical and basipetal flow. For the present study, internodal cells that had not yet started to elongate were generally too small or inaccessible to microinject but loading of internodal cell primordia through leakage from nearby injected cells allowed visualization of F-actin (Fig. 1). More clearly defined arrays were observed in internodal cell primordia by immunofluorescence after whole cell fixation (Fig. 2). In such internode primordia, actin was arranged in a reticulate network throughout the cytoplasm and was closely associated with the single central nucleus (Figs. 1 and 2), similar to the arrangement of actin in densely cytoplasmic higher plant cells (Traas et al. 1987, Seagull et al. 1987). In cells just beginning to elongate, injection of fluorescent phallotoxin (Fig. 3) and immunofluorescence (Fig. 4) revealed axial polarization of actin bundles. Although the actin bundles in these young cells were only roughly parallel to one another and frequently crossed over (Fig. 3 a) or merged (Fig. 4), the bundles never appeared discontinuous, even at the cell ends where they changed orientation by 180° (Fig. 3 b). Chloroplasts were also only arranged in a loosely axial pattern (not shown) but no close association between actin bundles and chloroplast files was observed. At this stage, the formation of the large central vacuole is incomplete and fluorescent phallotoxin injection localized actin bundles within transvacuolar strands of living cells (Figs. 1 and 5).

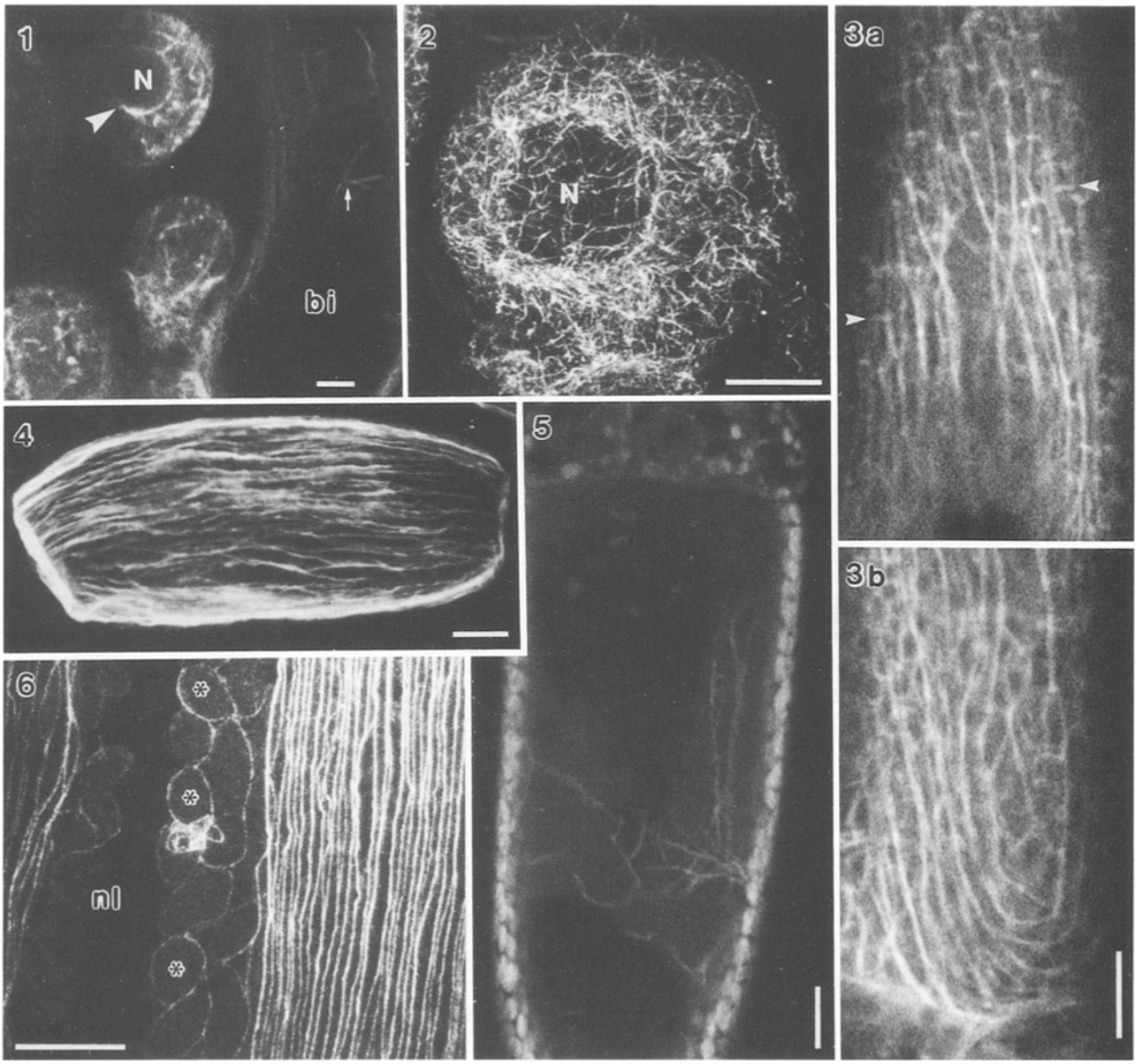

Fig. 1–6. Actin filament distribution during early development of characean internodal cells. Bars: 10 μm

Fig. 1. Living axial (from main axis) and lateral branch (axillary) primordia of *N. pseudoflabellata* labelled with FITC phalloidin. Phalloidin was injected into a large subjacent internode and has moved, presumably through plasmodesmata, into several nearby cells including an elongating branchlet internode (*bi*) in which F-actin is visualized in the transvacuolar strands (arrow). In the primordia, actin bundles form perinuclear cages (arrowhead; *N* location of nucleus) and cytoplasmic networks. Single image scan

Fig. 2. Glutaraldehyde-fixed branchlet internode primordium of *N. pseudoflabellata*. Anti-actin immunofluorescence reveals abundant perinuclear (*N* location of nucleus) and cytoplasmic actin bundles. Projection of 10 serial images collected at 0.42 μm intervals

Fig. 3. *N. pseudoflabellata* branchlet internode at start of elongation. Bodipy phallacidin microinjection. **a** Towards tip. **b** At base of same cell, showing change of actin bundle direction. Subcortical actin bundles are longitudinally oriented but are still relatively disorganized. Cortical actin (arrowheads) is also visible. Single image scan

Fig. 4. Anti-actin immunofluorescence of a fixed *C. corallina* branchlet internode at early elongation stage. Projection of 16 serial images collected at 0.33 μm intervals

Fig. 5. Mid-plane focus of FITC phalloidin-microinjected *N. pseudoflabellata* branchlet internode. Actin bundles are visible in endoplasm and through transvacuolar strands

Fig. 6. Anti-actin immunofluorescence of a fixed *N. pseudoflabellata* axial internode. As elongation progresses, subcortical actin bundles are aligned parallel to one another but are not yet organized in groups along chloroplast files. In neutral line (*nl*), actin associates closely with the loosely organized chloroplasts (*). Projection of 16 serial images collected at 0.5 μm intervals

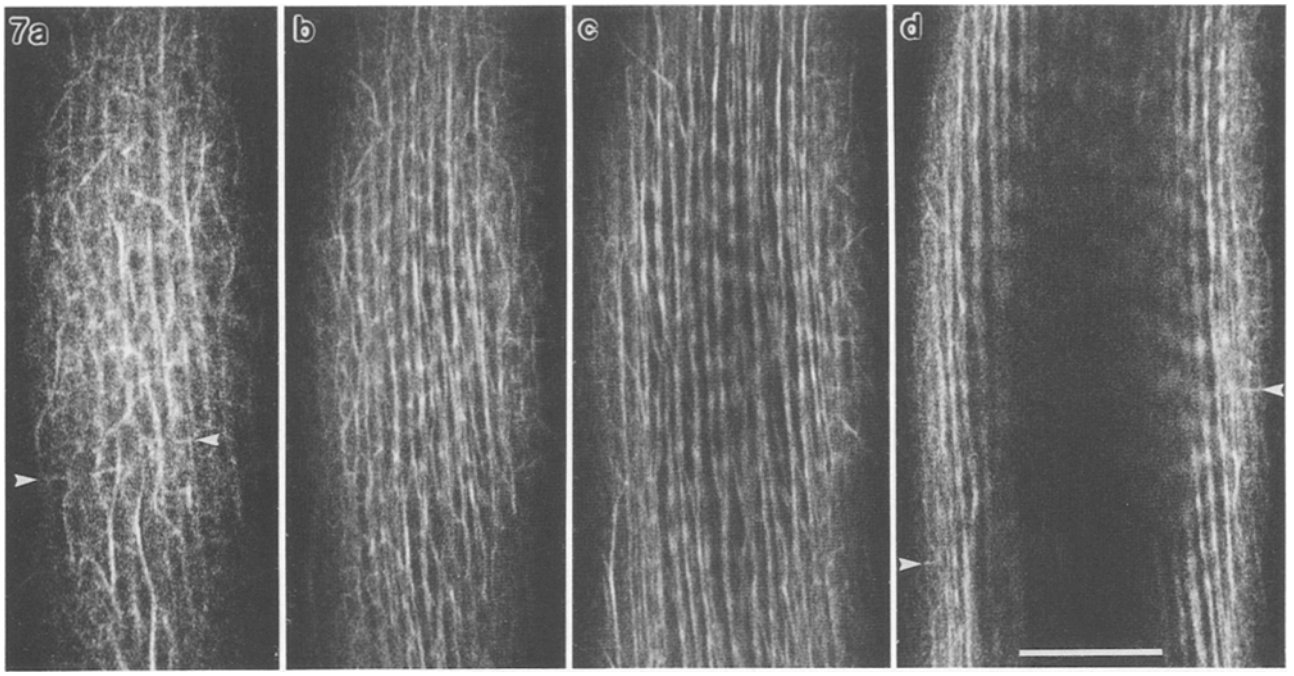

Fig. 7. Optical sectioning through cortex of a *Nitella pseudoflabellata* axial internode injected with FITC-phalloidin. Bar: 20 µm. **a** Cortex (= 0 µm), **b** –1.6 µm, **c** –2.0 µm, **d** –3.2 µm. Note that compared to the parallel arrangement of subcortical bundles, the cortical bundles, evident in **a**, are loosely organized and of wavy appearance. Some transverse cortical actin elements are visible (arrowheads) and especially obvious in **d** near the edge of the photograph

As internodal cells expand, the chloroplasts are first arranged in longitudinally oriented files but these files gradually become aligned at a small angle relative to the longitudinal axis. This realignment is caused by a gradual twisting of the cortex and cell wall, and reflects the major axis of strain deformation. It is particularly evident in the internodes that make up the frond's central axis so that, eventually, the endoplasmic organelles follow a helical path as they circumnavigate the internode. Branchlet internodes at whorls have less tendency to twist in this fashion and the chloroplast-free strips lying between opposing flows of endoplasm, known as neutral lines, may extend the length of the cell without significant deviation from the long axis. The results of the present study indicate that actin bundles become increasingly organized as internodal cells begin elongating, first becoming parallel to one another and evenly spaced (Fig. 6) and only later organized as discrete sets of bundles along each chloroplast file (Fig. 17). Such eventual close adherence of actin bundles along chloroplast files can be observed in both living, actively streaming, phalloidin-injected cells (Figs. 8–12) and in fixed cells (Figs. 14 b and 15–17).

Cortical actin strands

The prominent actin bundles located along the internal face of the chloroplast files are defined as subcortical actin bundles because they lie at the interface between the motile endoplasm and the stationary cell cortex. Actin bundles also extend from the subcortex through the chloroplast layer toward the cell periphery. This reticulate "cortical actin bundle" network, which could be visualized by phalloidin microinjection (Fig. 7), is more extensive than that described by Williamson et al. (1986) by immunofluorescence. Fluorescent phalloidin occasionally labelled finer F-actin elements near the plasma membrane (Figs. 7–9), which we term cortical actin strands. In contrast to the cortical actin bundles, whose orientation is approximately longitudinal, these finer elements were mostly transversely oriented (Fig. 9). Cortical actin strands were also preserved in fixed cells (Figs. 14 a, 16 and 17) and immunofluorescence generally revealed a much more extensive network of them than did phalloidin microinjection. Procedures for vacuolar perfusion fixation used in previous studies (Wasteneys and Williamson 1991)

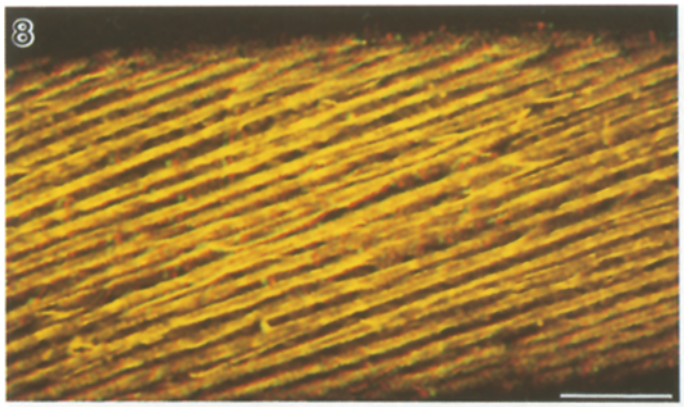
8

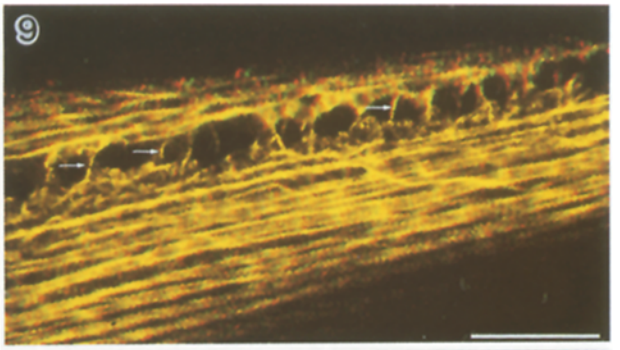
9

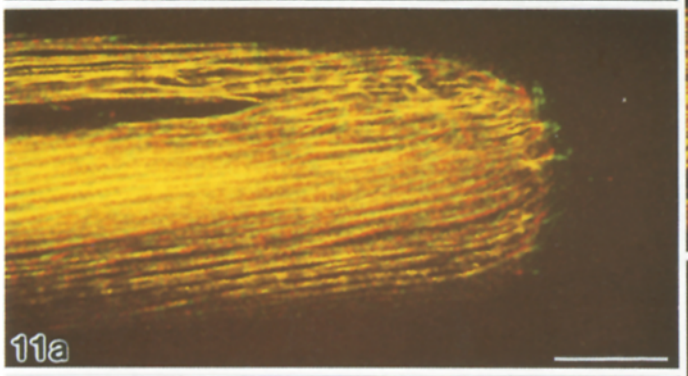
11a

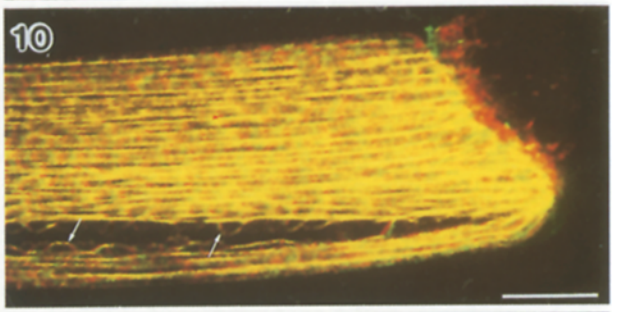
10

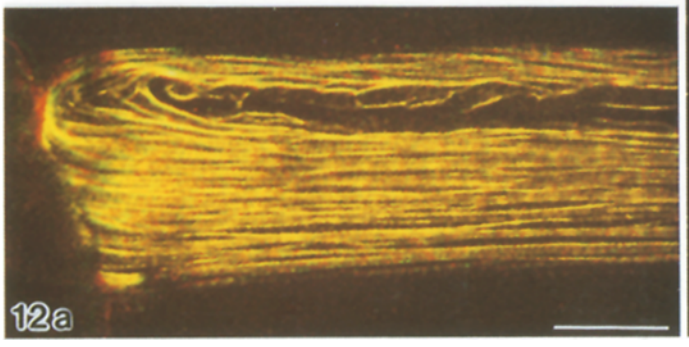
12a

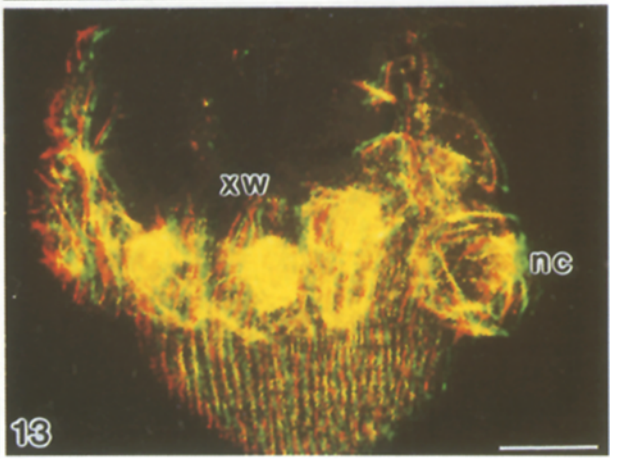
xw
nc
13

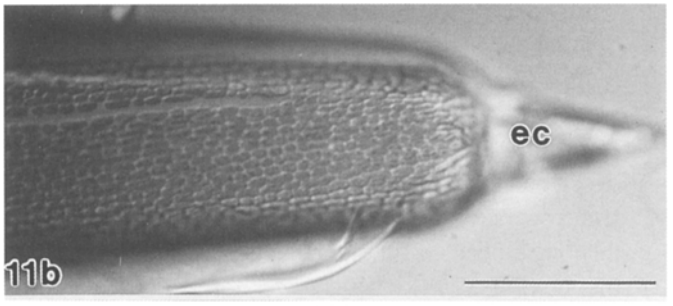
ec
11b

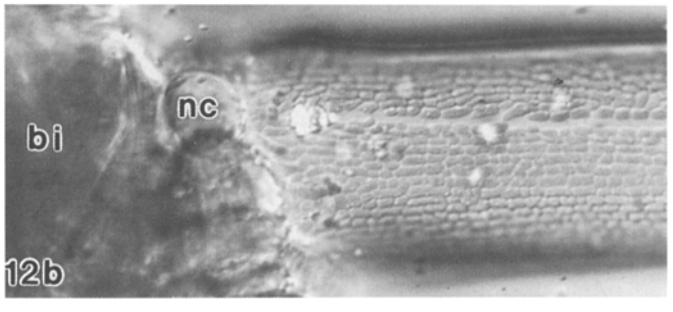
nc
bi
12b

did not preserve cortical actin strands. On the other hand, by modifying the technique to ensure continuation of streaming during a brief pre-fixation perfusion, some cortical actin strands were preserved, though only in the region of the neutral line (Fig. 16). Whole cell fixation was therefore judged to be superior to perfusion fixation for reliable preservation of cortical actin strands.

Chloroplast actin rings and actin bundles at the neutral line

A novel feature observed in this study was the chloroplast actin ring, observable both by phalloidin microinjection (Figs. 10 and 12 a) and anti-actin immunofluorescence (Figs. 6, 15, 16, 17 a and 19). Rings were found on the chloroplasts bordering the neutral line. These chloroplasts are generally sparsely distributed and, unlike the chloroplasts overlying the streaming cytoplasm (see Fig. 17 b), tend to be rounded rather than elongate and lack actin bundles on their endoplasmic face. Rings lie parallel to the cell surface and are located at the (radial) mid-plane of the chloroplasts, a plane closer to the cell periphery than the subcortical actin bundles that generate streaming. In addition to the actin rings, longer bundles were frequently associated with the chloroplasts and/or the chloroplast actin rings. The arrangement of these bundles was quite variable but generally demonstrated a close association with chloroplasts. In Fig. 17, for example, actin bundles that lie along both sides of a chloroplast file (shown in Fig. 17 b) traverse the neutral line.

Microtubules at the neutral line

Anti-tubulin immunofluorescence showed that cortical microtubules are organized slightly differently at the neutral line than in regions above the chloroplasts and streaming endoplasm (Fig. 18). The microtubules deviated slightly from the general transverse alignment but appeared to be more uniformly aligned and, judging by the strength of fluorescent signal, were at least partially bundled. The 3-dimensional projection in Fig. 18 shows that the microtubule array, which presumably follows the contours of the plasma membrane, bulges outward at the neutral line.

Actin patterns at nodal zones

Subcortical actin bundles remain parallel at the ends of internodal cells, providing an uninterrupted track for the motile organelles. In a few internodal cell types located in the lateral branchlets, such as the penultimate dactyl cells (Fig. 11) and other junctions lacking nodal cells (Fig. 19), chloroplast files continue around the ends of cells and actin bundles follow the same course as the chloroplast files. The end walls of many internodal cells, including those of the main axis, however, lack chloroplast files. Despite this, actin bundles remain parallel and are evenly spaced with considerable precision (Figs. 13 and 20), thereby demonstrating that the mechanism that organizes actin bundles does not depend on the existence of chloroplast files. Organization of microtubules, in contrast, is markedly different at cell ends compared to that along the longitudinal axis (Fig. 21). Very few

Figs. 8–13. Stereo anaglyphs of FITC-phalloidin-injected cells of *Nitella pseudoflabellata*. Bars: 25 μm

Fig. 8. Internode of main axis has helical subcortical actin bundles running in groups along chloroplast files. A few transverse cortical strands are also visible. Calculated from 11 serial images collected at 1 μm intervals

Fig. 9. At neutral line, transverse cortical actin strands are visible. Calculated from 10 serial images collected at 1.6 μm intervals

Fig. 10. Base of branchlet internode at junction with main axis. Actin bundles merge at acute angle. Chloroplast actin rings are evident along edge of neutral line. Calculated from 26 serial images collected at 0.96 μm intervals

Figs. 11 a and **12 a.** Dactyl cell at tip of branchlet

Fig. 11 a. At tip of cell, actin bundles continue around end along chloroplast files which persist beneath the dactyl end cell (not labelled) and the neutral line narrows at an acute angle. Calculated from 20 serial images collected at 0.96 μm intervals

Fig. 12 a. At base of same cell, actin bundles change direction with a U-bend. Calculated from 16 serial images collected at 0.64 μm intervals

Fig. 13. Multicellular node of main axis. The internodal cell cross wall is devoid of chloroplasts but actin bundles continue in parallel around cell end. Some actin bundles in nodal cells are also labelled by transfer of phalloidin from the injected internodal cell. Calculated from 21 serial images collected at 0.48 μm intervals

Figs. 11 b and **12 b.** Differential interference contrast video images of injected dactyl cell corresponding to anaglyphs Figs. 11 a and 12 a. Bar: 100 μm

Fig. 11 b. Chloroplast files continue around the apex of this dactyl cell, which joins the conical dactyl end cell (*ec*; out of focus)

Fig. 12 b. The base of the cell attaches to a multicellular node (*nc* nodal cell), below which lies a much larger branchlet internodal cell (*bi*)

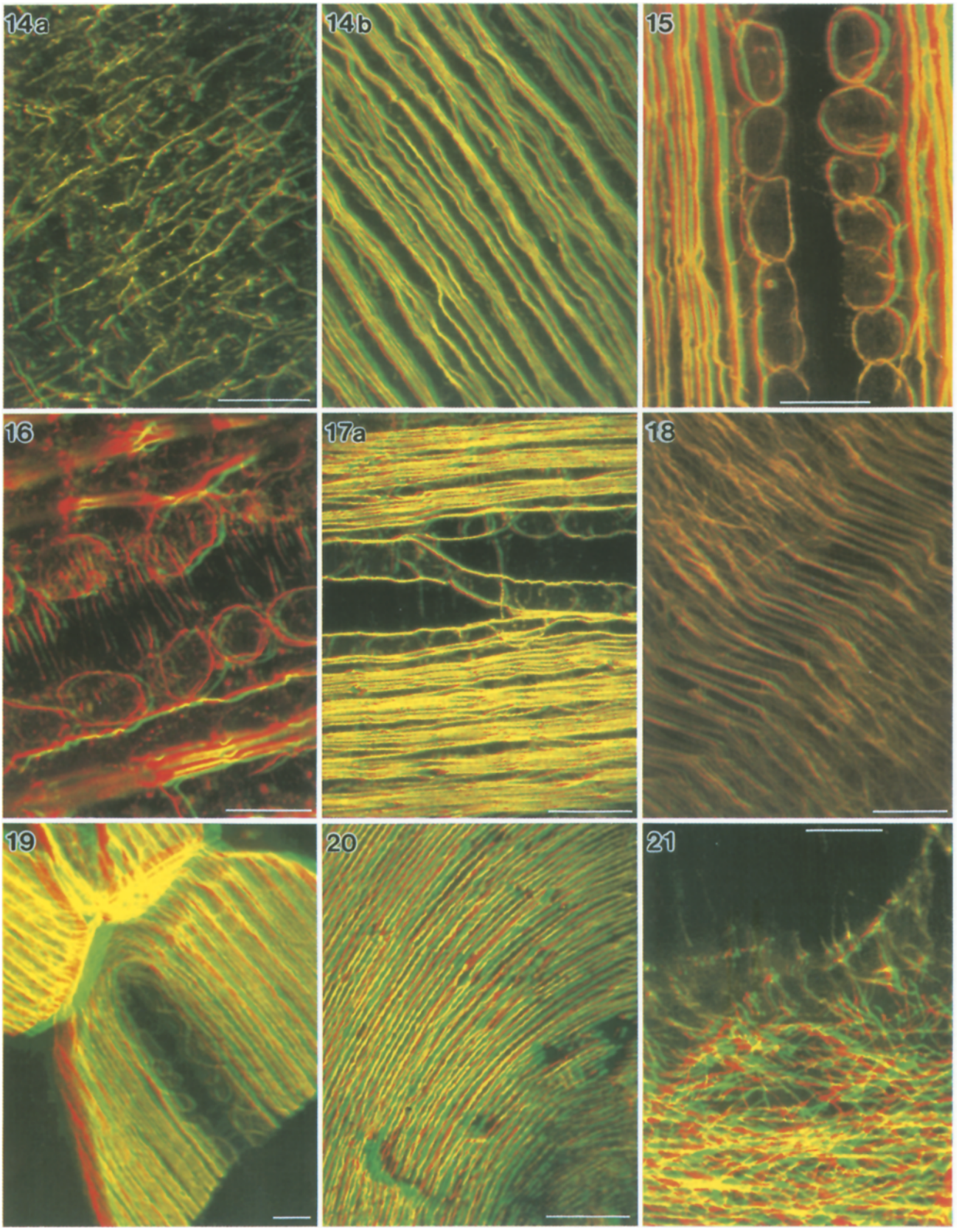
14a
14b
15
16
17a
18
19
20
21

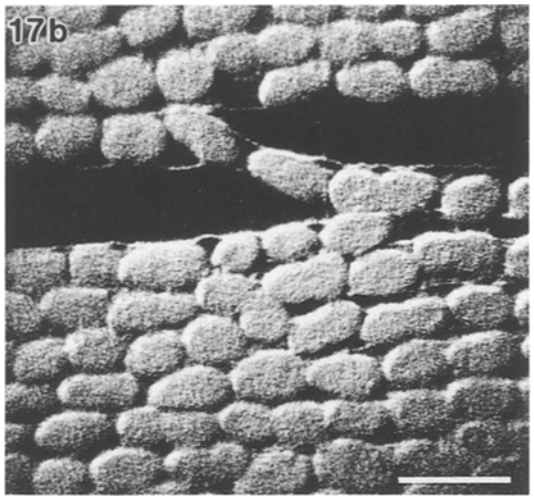

Fig. 17 b. Projection of confocal image of chloroplast autofluorescence from same area depicted in Fig. 17 a. Channels were adjusted to allow some bleeding from the FITC signal resulting in visibility of actin bundles as well as chloroplasts. Projection of 12 images collected at 0.3 μm intervals; bar: 10 μm

microtubules were localized at the end walls of internodal cells and orientation was also very different to that along the long axis. Towards the corner of the end wall, microtubules lose their predominantly transverse orientation and some microtubules align in the same direction as the actin bundles across the end wall.

Although we have not examined in detail the cytoskeleton of the relatively small cells of the multicellular nodal regions, actin bundles in these cells commonly labelled with the phallotoxins that had been injected into adjacent internodal cells (Fig. 13). These uninucleate cells contained a peripheral as well as peri-nuclear network of actin bundles.

The shift in direction of subcortical actin bundles at the cell ends is variable. Those actin bundles closest to the edge of the neutral line must be contorted through 180° in a short distance, and in some cases make a U-shaped turn such that the neutral line remains fairly open (Figs. 12 and 19). The shift in direction of bundles can be much more abrupt, with the neutral line narrowing to a point so that the bundles bend sharply through an acute angle (Figs. 10 and 11).

Discussion

By using both immunofluorescence after chemical fixation and injection of living cells with fluorescent

Figs. 14–21. Stereo anaglyphs from glutaraldehyde-fixed immunofluorescently labelled internodal cells. All images, except Fig. 16, are from material prepared by whole cell fixation. Figure 16 was prepared by the modified perfusion fixation method. Bars: 10 μm

Fig. 14. Two partial series from same original series showing cortical (**a**) and subcortical (**b**) actin in a branchlet internode of *C. corallina*. **a** Cortical actin strands are predominantly oriented perpendicular to the orientation of the subcortical bundles and the cell's long axis (diagonal to the long axis of the page). Calculated from first 10 images of series collected at 0.25 μm intervals. **b** Calculated from remaining 13 images collected at 0.25 μm intervals

Fig. 15. Neutral line region of a *N. pseudoflabellata* axial internode. Actin ring structures associate with virtually all the chloroplasts that border the neutral line. In contrast, actin rings are rarely observed on the chloroplasts organized into tight files overlying the streaming endoplasm. Calculated from 17 serial images collected at 0.25 μm intervals

Fig. 16. Neutral line region of a perfusion-fixed *C. corallina* axial internode. In addition to the chloroplast ring structures, this series extends into the cortex, where transverse cortical actin strands are visible. Perfusion fixation preserved cortical actin strands only at the neutral line. Calculated from 22 serial images collected at 0.29 μm intervals

Fig. 17 a. Neutral line region of a *N. pseudoflabellata* branchlet internode. Here, a file of chloroplasts (see equivalent chloroplast image, Fig. 17 b) crosses the neutral line and is bordered on both sides by actin bundles. Actin rings on some of the chloroplasts are also evident. Calculated from 12 serial images collected at 0.3 μm intervals

Fig. 18. Microtubules at neutral line in a *C. corallina* axial internode. The anaglyph is projected so that the viewer is looking out from the cell interior. Calculated from 24 serial images collected at 0.21 μm intervals

Fig. 19. Node between primary and secondary internodes of a *N. pseudoflabellata* branchlet. Note lack of nodal cells at this junction. Subcortical actin bundles continue around cell ends making a U-bend near the neutral line. Note actin rings on chloroplasts adjacent to neutral line. Calculated from 26 serial images collected at 0.42 μm intervals

Fig. 20. Actin bundles at end wall of a *C. corallina* axial internode. Here actin bundles are evenly spaced, unlike in the rest of the cell where they are arranged in groups along chloroplast files (Fig. 14 b). Despite lack of chloroplast files, actin bundles remain parallel to one another as they undergo a shift in orientation. Calculated from 16 serial images collected at 0.25 μm intervals

Fig. 21. Microtubules at corner between transverse wall and end wall of a *C. corallina* axial internode. In lower part of image, which shows the longitudinal (side) wall of the cell, microtubules are broadly transverse. At the corner of the side and end walls, microtubules become scarce and those present are aligned in the same direction as the actin bundles, approximately perpendicular to microtubule orientation along the side wall. Calculated from 33 serial images collected at 0.33 μm intervals

phallotoxins, we have found hitherto unsuspected similarities between the organization of actin in developing characean internodal cells and higher plant cells. Most significant is the distinct array of actin strands in the cell cortex whose orientation, like cortical microtubules, is transverse in elongating cells. A novel feature is chloroplast-associated actin, in the form of ring structures and bundles, located alongside the neutral line.

Preserving actin in plant cells

Determining the full extent of F-actin in plant cells remains problematic. The conspicuous bundles of actin filaments associated with cytoplasmic streaming and organelle motility are relatively resistant to destabilization and thus are readily preserved by conventional fixation protocols. Subcortical actin bundles in characean internodal cells, for example, resist disassembly for extended periods during vacuolar perfusion experiments when cell ends are removed and an artificial cytoplasm is allowed to flow through the opened cell for tens of minutes (Williamson 1975, Shimmen and Tazawa 1982). In contrast, finer actin structures, whose presence in the plant cell cortex has been confirmed immunologically in densely cytoplasmic tissues (McCurdy et al. 1989) or in rapidly frozen, freeze-substituted material (Lancelle and Hepler 1989, Ding et al. 1991), are not preserved by conventional fixation of most plant cells and especially of those that are highly vacuolated. Numerous modified fixation and non-fixation procedures allow actin distribution to be probed more thoroughly in a variety of plant cell types. Improvements include the use of proteolytic inhibitors, actin-specific protectants like tropomyosin (Kakimoto and Shibaoka 1987) and the cross-linking reagent m-maleimidobenzoyl-N-hydroxy-succinimidester (MBS) prior to (Sonobe and Shibaoka 1989) or independent of aldehyde fixation (Cho and Wick 1991). We report elsewhere that pretreatment of *Nitella* internodal cells with MBS prior to aldehyde fixation preserves F-actin structures similar to those documented in this study (Collings et al. 1995).

Comparison of fixation methods

We compared various means of fixing cells to determine how best to preserve cortical actin. Our conventional approach to immunofluorescence by which the internodal cells are fixed after first removing the central vacuole (Williamson et al. 1989, Wasteneys and Williamson 1991) did not preserve cortical actin or the chloroplast rings. Minimizing the interruption to streaming by introducing an ATP-containing perfusion solution preserved only those cortical actin structures close to the neutral line, perhaps because they are reached more quickly by the internally perfused fixative than those cortical actin strands shielded from the endoplasm by chloroplasts. Fixing whole cells, however, preserved abundant cortical actin structures; the method minimized handling of material and allowed preservation of cells that would otherwise be too small for perfusion. Cytoskeletal organization at the end walls and in the nodal cells could also be examined because removal of the cell ends – a prerequisite for vacuolar perfusion – was not necessary. We obtained best results using 1% glutaraldehyde alone in fixation buffer; use of formaldehyde at concentrations high enough to preserve cells caused plasmolysis (Taylor 1988). Although we cannot attest to the completeness of the actin array that is preserved in glutaraldehyde, from the fact that the distribution matches or betters that observed in living cells with fluorescent phallotoxins, we conclude that actin can be preserved extremely well with glutaraldehyde. Similarly, whole cell fixation improved microtubule preservation. Perfusion fixation generally does not preserve cortical microtubules at the neutral line (Wasteneys and Williamson 1993) but microtubules were abundant at this location after whole cell fixation, in agreement with observation of living cells following microinjection of fluorescent tubulin (Foissner and Wasteneys 1994). Presumably the microtubules at the neutral line disassemble relatively easily during pre-fixation perfusion because they are not protected by the chloroplast layer. The key to the success of whole cell fixation for preserving both cortical actin and microtubules is likely to be the rapidity of penetration of the fixative to the cortical sites (Mersey and McCully 1978). Characean internodal cells are aquatic and thus lack cuticle which, in land plants, reduces the speed at which fixative penetrates cells. Thus, the contention that fine actin filaments are sensitive to glutaraldehyde fixation (Lehrer 1981) may reflect more the time it takes for glutaraldehyde to reach the actin filaments than disruptive effects of glutaraldehyde per se.

Phalloidin injection

Actin function was apparently unaltered by labelling with microinjected fluorescent phallotoxins because

streaming velocities were not reduced by the treatment. Similarly, labelling subcortical actin bundles with fluorescent phallacidin by perfusion did not reduce the velocity of artificially reactivated streaming in *Chara* internodal cells (Nothnagel et al. 1981). Kron and Spudich (1986) and more recently Kohne et al. (1992) have demonstrated that movement of actin filaments along solid-phase myosin substrates is not impeded by labelling of the actin with phallotoxin. It may be concluded, therefore, that the small size of phallotoxins (< 1250 Da) does not interfere with the binding to actin of many actin-based motor proteins. Nevertheless, cortical actin strands appeared to be much more extensive in fixed, immunolabelled tissue than in living, phallotoxin-injected cells (compare Figs. 8 and 14 a). Cortical actin strands might be destabilized in cells prepared for microinjection but it is also possible that detection of relatively weak signals is more difficult in living cells. The labelled cortical strands are not as bright as the subcortical bundles, probably because they contain relatively few actin filaments. Their relatively weak signal may be undetectable at detector settings adequate for the brighter subcortical bundles. The wide dynamic range in signal strengths seemed to be less of a problem with immunofluorescence, perhaps because higher laser intensity and longer dwell times could be used to record the full range of signal intensities without the photobleaching of fluorochromes that occurred in living tissue. Alternatively, phalloidin might bind less readily to cortical actin strands than it does to subcortical bundles. This could be caused by poor accessibility but phalloidin's small size (< 1250 Da) makes this an unlikely explanation. It is more likely that if phalloidin binds less readily to cortical actin that it is because of reduced affinity, reflecting distinct properties of cortical and subcortical actin. One further possible explanation for detection of relatively little cortical actin in phalloidin-injected cells is that phalloidin might cause aggregation of fine strands as reported by Sonobe and Shibaoka (1989). Compared to the cortical actin preserved by fixation (Fig. 14 a), the phalloidin-labelled actin in this study (Figs. 3, 7, and 8) does appear as short, thick elements, not dissimilar to the stable rods induced by cytochalasin treatment (see Collings et al. 1995). Our estimates of cytoplasmic phalloidin concentration, however, are approximately ten-fold less than those shown by Sonobe and Shibaoka (1989) to cause aggregation of actin. Despite its obvious value in studying actin distribution in living cells (Schmit and Lambert 1990, Cleary et al. 1992, Zhang et al. 1993, Meindl et al. 1994, Staiger et al. 1994), phalloidin should be considered a less than perfect reporter molecule.

Function of cortical actin strands

The function of cortical actin strands identified in this study remains uncertain. Their transverse orientation in elongating internodes predicts some relationship with the similarly aligned cortical microtubules but this relationship may be indirect. We have not yet explored in depth the nature of cortical microtubule-actin filament association but cytochalasin treatments do not change the orientation of cortical microtubules nor do they prevent reformation of a transverse microtubule array following drug-induced microtubule disassembly (Wasteneys unpubl.). Thus, cortical actin in characean internodal cells is unlikely to be involved in microtubule alignment. Some recent reports suggest a close association of actin with the plasma membrane and components of the cell wall in characean internodal cells. Foissner (1991) reported that cytochalasin B inhibits wound wall formation, implying involvement of F-actin in certain exocytotic events. Also, Wayne et al. (1992) provided indirect evidence that integrin homologues are active in *Chara* internodes. This would almost certainly require interaction of actin with the plasma membrane.

Development of subcortical actin bundle arrays

The axial organization of actin bundles arises in young internodal cells as soon as cell elongation becomes apparent and is probably a consequence rather than a cause of the establishment of cell polarity. It is suggested that the actin bundles and therefore the direction of streaming lie along the major axis of strain deformation (Green 1964) resulting in an off-axial helical orientation. Chloroplast files share this orientation pattern but there remains some uncertainty about the obligate nature of their association with subcortical actin bundles. Two observations made in this study suggest that actin bundles do not depend on the prepositioning of the chloroplasts for their alignment. First, during early elongation, when chloroplasts are still relatively disorganized, actin bundles are already arranged in well ordered, parallel arrays. Second, in agreement with SEM analysis of McLean and Juniper (1993), actin bundles remain parallel at the ends of cells where chloroplast files are absent.
The close association of actin with chloroplasts may therefore reflect a dependence of chloroplast align-

ment on actin bundle organization rather than vice versa. This is supported by earlier experimental approaches. Chen (1983) documented recovery of *Nitella* cells after centrifugation and noted that streaming patterns became established prior to alignment of chloroplasts along the same pathways. Williamson (1985) showed that detergent solubilization of chloroplasts in *Chara* does not remove actin bundles or alter their alignment significantly whereas a fibrous cortical meshwork, if released by trypsin, dislodges both actin bundles and chloroplasts. On the other hand, Green (1964) found that "the departure from oriented expansion in *Nitella* plastids when deprived of the normal strain environment takes place despite the fact that the streaming pattern is unchanged", suggesting that chloroplast alignment cannot be completely dependent on actin bundle organization.

The observation that actin bundles remain parallel at the ends of cells where chloroplast files are absent suggests that they are aligned by a mechanism other than strain deformation. Compared to the anisotropic growth of the internodal side walls, the end wall undergoes relatively little expansion during cell development. The precise order of the actin bundles at the nodal cross walls cannot, therefore, be attributed to strain alignment (Green 1964). Cytoplasmic flow, as demonstrated in experiments in which actin regeneration was documented in light-induced chloroplast-free windows, was suggested to align bundles across end walls (Williamson et al. 1984).

Significance of chloroplast actin rings

Rings of actin are evident on those chloroplasts nearest to the neutral line and, in many cases, longer bundles are also associated with these loosely strung chloroplasts. The chloroplasts lying along the edge of the neutral line could represent the establishment of new chloroplast files but, according to Green (1964), the number of chloroplast files is approximately constant over the course of development, the five-fold increase in average chloroplast size accounting for much of the increase in cell girth. Alternatively, the loosely strung chloroplasts and actin bundles bordering the neutral line could be a consequence of turbulent bulk flow due to boundary effects. Indeed, the chloroplast actin rings might be initially flow-aligned by neutral line turbulence and then participate in the motility of organelles in the neutral line. Williamson (1972) documented organelle movement along single fibrils (visible with differential interference contrast microscopy) and around chloroplasts adjacent to the neutral line in *Chara* and noted that organelles could move in opposite senses on neighbouring chloroplasts. The characean actin rings and bundles therefore appear to be capable of generating organelle motility.

The chloroplast actin rings might also serve to tether chloroplasts to other cortical structures. We have no experimental evidence for this but the involvement of actin in chloroplast migration and immobilization has been demonstrated in several plant and algal systems (Menzel and Schliwa 1986, Izutani et al. 1990, Wagner and Grolig 1992, Menzel 1994, Wada et al. 1993, Williamson 1993). Formation of actin rings on the plasma membrane side of chloroplasts in *Adiantum*, for example, is a feature of chloroplast immobilization (Kadota and Wada 1992). Characean chloroplasts may be stable but this does not preclude dependence on an active, albeit isometric, process to keep the chloroplasts in place. Interestingly, chloroplasts that accidentally become dislodged from the stationary cortical gel spin as they move with the streaming endoplasm (Kamiya 1962, Williamson 1972). The nuclei of *Nitella* also spin in this manner, an activity that has been attributed to the presence of actin rings; spinning of nuclei does not occur in *Chara*, whose nuclei lack actin rings (Wasteneys and Williamson 1991).

In conclusion, by improving visualization techniques, we revealed a much more extensive distribution of actin in characean internodal cells than has been previously described. Importantly, these findings show that characean actin is organized in a manner that is similar to that of higher plants. With this knowledge, it will be possible to more accurately determine the actin cytoskeleton's involvement in many developmental and physiological processes.

Acknowledgement

The phallotoxin injection work was carried out at ANU, during PKH's sabbatical in 1991–1992 and the immunofluorescence study was conducted at the Max-Planck-Institute for Cell Biology in Ladenburg, Federal Republic of Germany during GOW's fellowship in 1992–1993. GOW gratefully acknowledges receipt of a research fellowship from Alexander von Humboldt Foundation and a Queen Elizabeth II fellowship from the Australian Research Council. DAC was recipient of an Australian Post Graduate Award. PKH was supported by a Fulbright grant from the Australian-American Educational Foundation and a U.S. Department of Agriculture grant (91-37304-6832 now 94-37304-1180). We are especially grateful to Dr. Richard Williamson for many helpful discussions and comments on

this manuscript. GOW also thanks Professor Dr. Eberhard Schnepf (University of Heidelberg) and Professor Dr. Peter Traub (Max-Plank-Institute for Cell Biology, Ladenburg) for support and Drs. Markus Braun, Franz Grolig, and Susanne Liebe for many helpful suggestions. Special thanks to Eric Hines and co-workers at the CSIRO Microscopy Centre, Canberra, for allowing us to use their Leica confocal laser scanning microscope to process images originating in Ladenburg.

References

Allen NS (1974) Endoplasmic filaments generate the motive force for rotational streaming in *Nitella*. J Cell Biol 63: 270–287

Barak LS, Yocum RR, Nothnagel EA, Webb WW (1980) Fluorescence staining of the actin cytoskeleton in living cells with 7-nitro-2-oxa-1,3 diazole-phalloidin. Proc Natl Acad Sci USA 77: 980–984

Braun M, Sievers A (1994) Role of the microtubule cytoskeleton in gravisensing *Chara* rhizoids. Eur J Cell Biol 63: 289–298

Chen JCW (1983) Effects of elevated centrifugal field on the *Nitella* cell and postcentrifugation patterns of its cytoplasmic streaming and chloroplast files. Cell Struct Funct 8: 109–118

Cho S-O, Wick SM (1991) Actin in the developing stomatal complex of winter rye: a comparison of actin antibodies and Rh-phalloidin labelling of control and CB-treated tissues. Cell Motil Cytoskeleton 19: 25–36

Cleary AL, Gunning BES, Wasteneys GO, Hepler PK (1992) Microtubule and F-actin dynamics at the division site in living *Tradescantia* stamen hair cells. J Cell Sci 103: 977–988

Cole L, Coleman J, Kearnes A, Morgan G, Hawes C (1991) The organic anion transport inhibitor, probenecid, inhibits the transport of Lucifer Yellow at the plasma membrane and the tonoplast in suspension-cultured cells. J Cell Sci 99: 545–555

Collings DA, Wasteneys GO, Williamson RE (1995) Cytochalasin rearranges cortical actin of the alga *Nitella* into short, stable rods. Plant Cell Physiol 36: 765–772

Corti B (1774) Osservazioni microscopiche sulla treella e sulla circolzione del fluido in una pianta aquajuola. Lucca

Ding B, Turgeon R, Parthasarathy MV (1991) Microfilament organization and distribution in freeze substituted tobacco plant tissues. Protoplasma 165: 96–100

Foissner I (1991) Induction of exocytosis in characean internodal cells by locally restricted application of chlortetracycline and the effect of cytochalasin B, depolarizing and hyperpolarizing agents. Plant Cell Environ 14: 907–915

– Wasteneys GO (1994) Injury to *Nitella* internodal cells alters microtubule organization but microtubules are not involved in the wound response. Protoplasma 182: 102–114

Green PB (1964) Cinematic observations on the growth and division of chloroplasts in *Nitella*. Amer J Bot 51: 334–342

Grolig F, Williamson RE, Parke J, Miller C, Anderton BH (1988) Myosin and Ca^{2+}-sensitive streaming in the alga *Chara*: two polypeptides reacting with a monoclonal anti-myosin and their localization in the streaming endoplasm. Eur J Cell Biol 47: 22–31

Izutani Y, Takagi S, Nagai R (1990) Orientation movements of chloroplasts in *Vallisneria* epidermal cells: different effects of light at low and high fluence rates. Photochem Photobiol 41: 105–111

Jung G, Wernicke W (1991) Patterns of actin filaments during cell shaping in developing mesophyll of wheat (*Triticum aestivum* L.). Eur J Cell Biol 56: 139–146

Kachar B, Reese TS (1988) The mechanism of cytoplasmic streaming in characean algal cells: sliding of endoplasmic reticulum along actin filaments. J Cell Biol 106: 1545–1552

Kadota A, Wada M (1992) Photoinduction of formation of circular structures by microfilaments on chloroplasts during intracellular orientation in protonemal cells of the fern *Adiantum capillus-veneris*. Protoplasma 167: 97–107

Kakimoto T, Shibaoka H (1987) A new method for preservation of actin filaments in higher plant cells. Plant Cell Physiol 28: 1581–1585

Kamiya N (1959) Protoplasmic streaming. Springer, Wien [Heilbrunn LV, Weber F, et al (eds) Protoplasmatologia, vol 8, 3 a]

– (1962) Protoplasmic streaming. In: Ruhland W (ed) Encyclopedia of plant physiology, vol 17/2. Springer, Berlin Göttingen Heidelberg, pp 979–1035

Kersey YM, Hepler PK, Palevitz BA, Wessels NK (1976) Polarity of actin filaments in characean algae. Proc Natl Acad Sci USA 73: 165–167

Kohno T, Ishikawa R, Nagata T, Kohama K, Shimmen T (1992) Partial purification of myosin from lily pollen tubes by monitoring with in vitro motility assay. Protoplasma 170: 77–85

Kron SJ, Spudich JA (1986) Fluorescent actin filaments move on myosin fixed to a glass surface. Proc Natl Acad Sci 83: 6272–6276

Kuroda K (1990) Cytoplasmic streaming in plant cells. Int Rev Cytol 121: 267–307

Lancelle SA, Hepler PK (1989) Immunogold labelling of actin on sections of freeze-substituted plant cells. Protoplasma 150: 72–74

Lehrer SS (1981) Damage to actin filaments by glutaraldehyde: protection by tropomyosin. J Cell Biol 90: 459–466

Lessard JL (1988) Two monoclonal antibodies to actin: one muscle selective and one generally reactive. Cell Motil Cytoskeleton 10: 349–362

McCurdy DW, Sammut M, Gunning BES (1989) Immunofluorescent visualization of arrays of transverse cortical actin microfilaments in wheat root-tip cells. Protoplasma 147: 204–206

McLean B, Juniper BE (1988) Fine structure of *Chara* actin bundles, using rapid-freezing and deep etching. Cell Biol Int Rep 12: 509–517

– – (1993) The arrangement of actin bundles and chloroplasts in the nodal regions of characean internodal cells. Eur J Phycol 28: 33–37

Meindl U, Zhang D, Hepler PK (1994) Actin microfilaments are associated with the migrating nucleus and the cell cortex in the green alga *Micrasterias*. J Cell Sci 107: 1929–1934

Menzel D (1994) Dynamics and pharmacological perturbations of the endoplasmic reticulum in the unicellular green alga *Acetabularia*. Eur J Cell Biol 64: 113–119

Schliwa M (1986) Motility in the siphonous green alga *Bryopsis*. II. Chloroplast movement requires organized arrays of both microtubules and actin filaments. Eur J Cell Biol 40: 286–295

Mersey BG, McCully ME (1978) Monitoring the course of fixation in plant cells. J Microsc 114: 49–76

Nagai R, Rebhun LI (1966) Cytoplasmic microfilaments in streaming *Nitella* cells. J Ultrastruct Res 14: 571–589

Nothnagel EA, Barak LS, Sanger JW, Webb WW (1981) Fluorescence studies on modes of cytochalasin B and phallotoxin action on cytoplasmic streaming in *Chara*. J Cell Biol 88: 364–372

Palevitz BA, Ash JF, Hepler PK (1974) Actin in the green alga *Nitella*. Proc Natl Acad Sci USA 71: 363–366

Pickett-Heaps JD (1967) Ultrastructure and differentiation in *Chara* sp. Aust J Biol Sci 20: 539–551

Schmit A-C, Lambert A-M (1990) Microinjected fluorescent phalloidin in vivo reveals the F-actin dynamics and assembly in higher plant mitotic cells. Plant Cell 2: 129–138

Seagull RW, Falconer M, Weerdenburg CA (1987) Microfilaments: dynamic arrays in higher plant cells. J Cell Biol 104: 995–1004

Shimmen T, Tazawa M (1982) Reconstitution of cytoplasmic streaming in Characeae. Protoplasma 113: 127–131

Sonobe S, Shibaoka H (1989) Cortical fine actin filaments in higher plant cells visualized by rhodamine-phalloidin after pretreatment with m-maleimidobenzoyl N-hydroxysuccinimide ester. Protoplasma 148: 80–86

Staiger CJ, Yaun M, Valenta R, Shaw PJ, Warn RM, Lloyd CW (1994) Microinjected profilin affects cytoplasmic streaming in plant cells by rapidly depolymerizing actin microfilaments. Curr Biol 4: 215–219

Taylor DP (1988) Direct measurement of the osmotic effects of buffers and fixatives in *Nitella flexilis*. J Microsc 150: 71–80

Traas JA, Doonan JH, Rawlins DJ, Shaw PJ, Watts J, Lloyd CW (1987) An actin network is present in the cytoplasm throughout the cell cycle of carrot cells and associates with the dividing nucleus. J Cell Biol 105: 387–395

Wada M, Grolig F, Haupt W (1993) Light-oriented chloroplast positioning. J Photochem Photobiol B 17: 3–25

Wagner G, Grolig F (1992) Algal and chloroplast movements. In: Melkonian IM (ed) Algal cell modility. Chapman and Hall, New York, pp 39–72

Wasteneys GO, Williamson RE (1991) Endoplasmic microtubules and nucleus-associated actin rings in *Nitella* internodal cells. Protoplasma 162: 86–98

– – (1993) Cortical microtubule organization and internodal cell maturation in *Chara corallina*. Bot Acta 106: 136–142

– Gunning BES, Hepler PK (1993) Microinjection of fluorescent brain tubulin reveals dynamic properties of cortical microtubules in living plant cells. Cell Motil Cytoskeleton 24: 205–213

Wayne R, Staves MP, Leopold AC (1992) The contribution of the extracellular matrix to gravisensing in characean cells. J Cell Sci 101: 611–623

Williamson RE (1972) Studies on cytoplasmic streaming and translocation. PhD thesis, University of Cambridge, Cambridge, UK

– (1974) Actin in the *Chara corallina*. Nature 248: 801–802

– (1975) Cytoplasmic streaming in *Chara*: a cell model activated by ATP and inhibited by cytochalasin B. J Cell Sci 17: 655–668

– (1985) Immobilisation of organelles and actin bundles in the cortical cytoplasm of the alga *Chara corallina* Klein ex. Wild. Planta 163: 1–8

– (1992) Cytoplasmic streaming in characean algae: mechanism, regulation by Ca^{2+}, and organization. In: Melkonian M (ed) Algal cell motility. Chapman and Hall, New York, pp 73–98

– (1993) Organelle movements. Annu Rev Plant Physiol Plant Mol Biol 44: 181–202

– Ashley CC (1982) Free Ca^{2+} and cytoplasmic streaming in the alga *Chara*. Nature 296: 647–651

– Toh BH (1979) Motile models of plant cells and the immunofluorescent localization of actin in a motile *Chara* cell model. In: Hatano S, Ishikawa H, Sato H (eds) Cell motility. Molecules and organization. Tokyo University Press, Tokyo, pp 339–346

– Hurley UA, Perkin JL (1984) Regeneration of actin bundles in *Chara*: polarized growth and orientation by endoplasmic flow. Eur J Cell Biol 34: 221–228

– Perkin JL, McCurdy DW, Craig S, Hurley UA (1986) Production and use of monoclonal antibodies to study the cytoplasm and other components of the cytoplasm of *Chara*. Eur J Cell Biol 41: 1–8

– Grolig F, Hurley UA, Jablonski PP, McCurdy DW, Wasteneys GO (1989) Methods for studying the plant cytoskeleton. In: Liskens HF, Jackson JF (eds) Plant fibers. Springer, Berlin Heidelberg New York Tokyo, pp 203–218 [Liskens HF, Jackson JF (eds) Modern methods of plant analysis, NS, vol 10]

Zhang D, Wadsworth P, Hepler PK (1993) Dynamics of microfilaments are similar, but distinct from microtubules during cytokinesis in living, dividing plant cells. Cell Motil Cytoskeleton 24: 151–155